e-Navi

Available online at http://www.e-navigation.kr/
e-Navigation Journal

Original article

Hyperbolic Tangent-Based Adaptive Neural Network Ship Heading Control

DING Shengda[a*], ZHAO Zijun[b], CHANG Qing[c]

[a*]School of Navigation and Shipping, Shandong Jiaotong University, China, 1517026939@qq. com

[b]School of Navigation and Shipping, Shandong Jiaotong University, China, 1481725038@qq. com

[c]School of Marine Engineering, Dalian Maritime University, China, changqing@sdjtu. edu. cn

Abstract

To address the issue of low heading tracking efficiency caused by nonlinear dynamic characteristics in ship heading motion, this paper proposes a neural network-based adaptive hyperbolic tangent control method for ship heading. By designing a second-order system robust controller, a saturated auxiliary design system is introduced into the regulator for direct internal compensation, enhancing the system's anti-interference capability under complex operating conditions. Meanwhile, hyperbolic tangent nonlinear modification is incorporated into the control strategy to optimize the output characteristics of control signals. The controller adopts a backstepping approach to design virtual control laws for trajectory tracking and utilizes the Radial Basis Function (RBF) of neural networks to approximate the uncertain parts of the ship model. The control algorithm is simulated and tested in the MATLAB environment, and its tracking effect is analyzed. Simulation results show that the control algorithm can ensure the stability of the closed-loop system under conditions of dynamic changes in system parameters, external disturbances, and uncertainties, and effectively solve the nonlinear problems in ship traffic control during trajectory tracking. The controller is designed concisely, meets the requirements of engineering practice, improves ship maneuverability, and has reference value for ship control.

Key words: adaptive control; neural networks; hyperbolic tangent; input saturation

https://doi.org/10.52820/j.enavi.2025.25.015

1. Introduction

The heading control of ships, as a core technology ensuring the safety and precision of maritime navigation tasks, has developed in close connection with advances in navigation equipment and control theory. In the 1920s, Anschutz and Sperry achieved a key breakthrough by developing a mechanical heading control system based on a shipborne gyrocompass, laying the engineering foundation for modern heading control (Xu and Zhang, 2013). With the introduction of PID control technology, the accuracy of heading control improved significantly; however, the robustness of such systems remained challenged by modeling errors in ship dynamics (Sun, 2020). To address modeling uncertainties and nonlinear dynamic characteristics under complex sea conditions, adaptive autopilots based on adaptive control theory were introduced (Du, 2020). By incorporating optimal control algorithms, model reference adaptive algorithms, and Kalman filtering techniques (Mu, 2019), the dynamic response capability of ship control systems was further enhanced.

Liu et al. (2024) addressed the problem of input saturation constraints by designing a heading controller that combines the backstepping method with a Lyapunov-based approach. Since the traditional backstepping method often suffers from the "explosion of complexity", Liu et al. (2022) proposed the Dynamic Surface Control (DSC) technique, which, in combination with fuzzy logic algorithms, effectively mitigates this issue. Neural networks, through their multilayer nonlinear structures, can automatically extract vessel motion features and construct approximate models of nonlinear motion under wind, wave, and current disturbances, thereby greatly advancing the development of ship control technology (Le, 2021). Zhou et al. (2024) introduced a first-order low-pass filter in the design process of dynamic surface control (DSC) to solve the curse of dimensionality caused by repeated differentiation and proposed an adaptive dynamic surface tracking controller based on neural networks (NN) to achieve tracking control. Zhang et al. (2025) incorporated integral sliding mode control and RBF neural networks to approximate lumped disturbances, and used a hyperbolic tangent saturation function with adjustable parameters to improve the robustness of the system. Liu et al. (2024) proposed a new fixed-time smooth estimation system to enhance the estimation performance of RBFNNs, and introduced the hyperbolic tangent function to effectively avoid the singularity problem of the derivative of the virtual controller. Jia et al. (2024) constructed a virtual desired sideslip (VDS) angle and introduced the hyperbolic tangent function to prevent instability or oscillations caused by non-smooth controllers. Ning et al. (2021) used the hyperbolic tangent function to design the expected hemispherical angle equation for solving the problem of ship curved trajectory tracking control, and combined backstepping with DSC technology for ship heading control. Suyama et al. (2024) introduced the hyperbolic tangent function and auxiliary variables to handle input constraints. Xu et al. (2024) proposed a new adaptive ship heading control law based on a hyperbolic tangent function. Zhang et al. (2021) adopted the hyperbolic tangent function to design the sliding surface and used the sliding mode control method to control the motion trajectory.

Most of the above methods are based on the assumption of mild environmental disturbances. However, in practical navigation, ships often operate in complex and dynamic environments, where existing methods still face limitations in balancing system response speed and tracking accuracy.

To address the challenge of balancing system response and tracking accuracy under complex and dynamic conditions, this paper proposes a neural network–based adaptive hyperbolic tangent control algorithm for ship heading control with input saturation constraints. The proposed design is based on a second-order system, embedding a saturation auxiliary system into the regulator's internal compensation loop to enhance disturbance rejection. Meanwhile, a hyperbolic tangent nonlinear modification is introduced into the control strategy

to construct a fully nonlinear regulation mechanism that covers the intermediate positive-definite function and the final control law. A virtual control law is designed via the backstepping method to achieve trajectory tracking, and an RBF neural network is employed to approximate system uncertainties, forming a concise yet robust control framework. Simulation results demonstrate that the proposed algorithm significantly improves heading tracking accuracy and response speed under complex conditions such as parameter variations and external disturbances, providing a new approach for nonlinear ship control problems.

2. Problem Analysis

2.1. Mathematical Model of the Ship Heading Contr ol System

In this paper, based on the Nomoto model, a second-order response model is established by integrating the motion control requirements and dynamic characteristics of the ship. Considering the effects of environmental disturbances such as wind, waves, and currents on ship motion, and incorporating rudder angle input as a control factor, a state-space representation of the ship's heading system is constructed. This provides a theoretical foundation for the study of ship heading control strategies.

The ship heading system model proposed by Nomoto is expressed as follows (Jia and Yang, 1997):

$$\ddot{\phi}+\frac{1}{T}H\left(\dot{\phi}\right)=\frac{K}{T}\delta \tag{1}$$

Among them, δ is the steering angle, ϕ is the heading angle, K is the curvature coefficient, and T is the following coefficient. $H\left(\dot{\phi}\right)$ is a nonlinear function of $\dot{\phi}$, which can be approximately expressed as:

$$H\left(\dot{\phi}\right)=a_1\dot{\phi}+a_2\dot{\phi}^3+a_3\dot{\phi}^5+\cdots \tag{2}$$

Among them, a_i , $i=1,2,3\cdots i$ are real constants.

During the simulation stage, physical constraints can be neglected. However, in actual navigation, the ship's motion must strictly comply with the operating limits of onboard equipment and navigation safety requirements.

The feasible range of the system input—the rudder angle δ —is $[-35^{\circ},+35^{\circ}]$. Among these, negative values correspond to port rudder angles, and positive values correspond to starboard rudder angles. The allowable range of the ship's yaw rate is defined as $[-3^{\circ}/s,+3^{\circ}/s]$. Therefore, input saturation and constraints are introduced in the controller design.

When the ship's navigation is controlled within limits, the small heading deviation allows the nonlinear terms to be approximated linearly, and thus the nonlinear coefficients $a_i(i=2,3,...)=0$. However, due to the nonlinear effects introduced by the actual steering mechanism, this linearization assumption does not always hold, and $a_i(i=2,3,...)$ cannot be assumed to be zero.

To establish a more suitable control model, this study considers a generalized nonlinear expression.

2.2 Compensatory Auxiliary System within the Controller

Due to the physical limitations of the steering engine, the ship's rudder angle input is subject t o range constraints. Command overruns can affe ct control performance and system stability. The refore, it is necessary to introduce an auxiliary system to compensate for the limited rudder ang le input. By monitoring and adjusting the contro l signal in real time, the command is corrected when the rudder angle saturates, thereby optimiz ing the control effectiveness of the steering engi ne. Consider the rudder angle constraints with m

aximum ($u_{\max}$) and minimum ($-u_{\min}$) input value s (the maximum rudder angle amplitude of the ship is 35°).

$$-u_{\min} \le u \le u_{\max} \tag{3}$$

$$u = sat(v) = \begin{cases} u_{\max}, & v > u_{\max} \\ v, & -u_{\min} \le v \le u_{\max} \\ -u_{\min}, & v < -u_{\min} \end{cases} \tag{4}$$

Among them, v denotes the control input to be designed for the system.

Accounting for the effects of input saturation, the system is structured as follows:

$$\dot{e} = \begin{cases} -c_{21}e - \dfrac{f(\cdot)}{e^2}e + (u - v), & |e| \ge \varepsilon \\ 0, & |e| < \varepsilon \end{cases} \tag{5}$$

Among them, e is an error term introduced by the auxiliary system to compensate for saturation effects, $c_{21} > 0$ is an adjustable parameter, and $z_2 = x_2 - a_2$ is an error variable. $f(\cdot) = f(z_2, \Delta u) = |z_2 \cdot b \cdot \Delta u| + \dfrac{1}{2}\Delta u^2$, $\Delta u = u - v$, ε is a designable positive parameter.

2.3. Radial Basis Function (RBF) Neural Network

Building upon the control design developed for ship course systems with known dynamics and parametric uncertainties under input saturation, this section addresses nonlinear systems containing uncertain nonlinearities by designing an adaptive control method based on neural networks.

In this paper, the RBF neural network is employed to approximate continuous functions.

$$\begin{aligned} &h(Z): R^q \to R \\ &h_{nn}(Z) = \theta^{\mathrm{T}}\xi(Z) \end{aligned} \tag{6}$$

Among them, the input vector is $Z \in \Omega_Z \subset R^q$, the weight vector is $\theta = [\theta_1, \theta_2, \ldots \theta_l]^{\mathrm{T}} \in R^l$, the number of NN nodes is $l > 1$, and $\xi(Z) = [\xi_1(Z), \xi_2(Z), \ldots, \xi_l(Z)]^{\mathrm{T}}$. Typically, $\xi_i(Z)$ is chosen as the Gaussian function, given as follows:

$$\xi_i(Z) = \exp\left[\frac{-(Z - \mu_i)^{\mathrm{T}}(Z - \mu_i)}{\eta_i^2}\right], i = 1, 2, \ldots, l \tag{7}$$

Among them, in the Gaussian function, $\mu_i = [\mu_{i1}, \mu_{i2} \ldots, \mu_{iq}]^{\mathrm{T}}$ represents the center position of the function, while η_i denotes its width.

$$h(Z) = \theta^{*\mathrm{T}}\xi(Z) + \delta^*, \forall Z \in \Omega_Z \tag{8}$$

Where θ^* is the ideal constant weight, and δ^* is the approximation error. For all $Z \in \Omega_Z$, when $\delta_m > 0$, there exists an ideal constant weight θ^* such that $|\delta^*| \le \delta_m$.

Among them, θ^* is a man-made defined quantity. θ^* is the value of θ that, for all $Z \in \Omega_Z \subset R^q$, minimizes $|\delta^*|$, that is,

$$\theta^* \triangleq \arg\min_{\theta \in R^l}\left\{\sup_{Z \in \Omega_Z}|h(Z) - \theta^{\mathrm{T}}\xi(Z)|\right\} \tag{9}$$

2.4. Introduction of the Hyperbolic Tangent Function

The hyperbolic tangent function is the ratio of the hyperbolic sine function ($\sinh x$) to the hyperbolic cosine function ($\cosh x$):

$$\tanh x = \frac{\sinh x}{\cosh x} = \frac{e^x - e^{-x}}{e^x + e^{-x}} \tag{10}$$

Among them, the graph of the hyperbolic tangent lies between the horizontal lines $y = 1$ and $y = -1$, that is, the range of the hyperbolic tangent function is $(-1, 1)$.

Derivation of State-Space Equations for Ship Heading Control System: Let $x_1 = \phi$, $x_2 = \dot{\phi}$, $u = \delta$ represent the ship's heading, heading rate of change, and input rudder angle, respectively. In ship heading control, affected by marine environmental factors and internal factors, external disturbances inevitably exist and exhibit random time-varying characteristics. Based on Equations (1) and (2), after introducing a comprehensive disturbance term into

the state-space expression, the mathematical model of the nonlinear ship control system considering actual operating conditions is obtained as follows:

$$\begin{cases} \dot{x}_1 = x_2 \\ \dot{x}_2 = f_1(x_1) + bu + d \\ y = x_1 \end{cases} \tag{11}$$

Among them, $f_1(x_1)$ is an unknown nonlinear function, $b = \frac{K}{T}$ is the control gain, y is the system output heading, and d is an unknown external disturbance that satisfies the aforementioned conditions.

Assumption 1 In the control system, the reference signal $y_d(t)$ is smooth and bounded, and its second-order derivative is continuously bounded. That is, there exists a positive constant B_0 such that the set $\prod_0 := \{(y_d, \dot{y}_d, \ddot{y}_d) : y_d^2 + \dot{y}_d^2 + \ddot{y}_d^2 \le B_0\}$ holds.

Assumption 2 There exists an upper bound for the uncertain term d, there is an unknown positive constant $|d^*|$ satisfying $d \le |d^*|$.

3. Controller Design

In modern control theory and engineering applications, input saturation is a common issue in practical control systems, which may affect system performance and even lead to instability. Designing adaptive control algorithms considering input saturation using the backstepping method is an important research direction. Based on mathematical derivation and stability analysis, the design process includes two core steps: first, select a Lyapunov function to design an intermediate control law, and utilize the characteristics of its derivative to construct a virtual control quantity that ensures the stability of the local subsystem; second, based on the intermediate control law and combined with actual constraint conditions, propose the actual control law to achieve stable control and performance optimization of the closed-loop system. The specific design steps are as follows:

*Step*1 : Define error variables

$$z_1 = x_1 - y_d \tag{12}$$

Taking the derivative of z_1, we have:

$$\dot{z}_1 = x_2 - \dot{y}_d \tag{13}$$

Given a compact set $\Omega_{x1} \in R^1$, let θ_1^* and δ_1^* be defined for any $x_1 \in \Omega_{x_1}$ as:

$$h_1(Z_1) = f_1(x_1) + d = \theta^{*\mathrm{T}} \xi_1(Z_1) + \delta_1^* \tag{14}$$

Among them, $Z_1 \overset{\Delta}{=} [x_1, \dot{y}_d]^{\mathrm{T}} \subset R^2 \frac{n!}{r!(n-r)!}$.

Select the virtual control law:

$$\alpha_2 = -c_1 \tanh(\frac{z_1}{\eta}) - \hat{\theta}^{\mathrm{T}} \xi_1(Z_1) + \dot{y}_d \tag{15}$$

Among them, $c_1 > 0$ is an adjustable parameter, and $\hat{\theta}$ is the estimated value of θ.

Substituting (15) into (13), we get:

$$\dot{z}_1 = -c_1 \tanh(\frac{z_1}{\eta}) - \hat{\theta}^{\mathrm{T}} \xi_1(Z_1) + z_2 \tag{16}$$

Select the Lyapunov function

$$V_1 = \frac{1}{2} z_1^2 \tag{17}$$

Taking the derivative, we have:

$$\dot{V}_1 = z_1 \dot{z}_1 \tag{18}$$

Substituting (16) into (18), we get:

$$\dot{V}_1 = -c_1 \tanh(\frac{z_1}{\eta}) \cdot z_1 + z_1 z_2 - z_1 \hat{\theta}^{\mathrm{T}} \xi_1(Z_1) \tag{19}$$

*Step*2 : Combining with (11), define the error variable:

$$z_2 = x_2 - \alpha_2 \tag{20}$$

Among them, α_2 is a virtual control law.

Taking the derivative of z_2, we have:

$$\dot{z}_2 = \dot{x}_2 - \dot{\alpha}_2 = \hat{\theta}^{\mathrm{T}} \xi_1(Z_1) + \delta_1^* + bu - \dot{\alpha}_2 \tag{21}$$

Considering the effect of input saturation of the system, according to (3), (4), and (5), a Lyapunov function is selected.

$$V_2 = V_1 + \frac{1}{2} z_2^2 + \frac{1}{2} \tilde{\theta}^{\mathrm{T}} \Gamma^{-1} \tilde{\theta} + \frac{1}{2} e^2 \tag{22}$$

Among them, $\tilde{\theta} = \theta - \hat{\theta}$ is the estimation error, $\hat{\theta}$ is the estimated value of θ, and Γ is a positive definite matrix. From (19) and (21), taking the

derivative of V_2, we have:

$$\begin{aligned}\dot{V}_2 &= -c_1 \tanh\frac{z_1}{\eta}\cdot z_1 + z_1 z_2 + z_2\dot{z}_2 - \tilde{\theta}^{\mathrm{T}}\Gamma^{-1}\dot{\hat{\theta}} + e\cdot\dot{e} \\ &\quad -z_1\hat{\theta}^{\mathrm{T}}\xi_1(Z_1) \\ &= -c_1 \tanh\frac{z_1}{\eta}\cdot z_1 + z_2[z_1 + \hat{\theta}^{\mathrm{T}}\xi_1(Z_1) + \delta_1^* + bu \\ &\quad -\dot{\alpha}_2] - \tilde{\theta}^{\mathrm{T}}\Gamma^{-1}\dot{\hat{\theta}} + e\dot{e} - z_1\hat{\theta}^{\mathrm{T}}\xi_1(Z_1)\end{aligned} \tag{23}$$

According to (5), we have:

$$e\dot{e} = -c_{21}e^2 - |z_2\cdot b\cdot\Delta u| - \frac{1}{2}\Delta u^2 + \Delta u e \tag{24}$$

According to Young's Inequality (Zhang, 2004)

$$\Delta u\cdot e \le \frac{1}{2}\Delta u^2 + \frac{1}{2}e^2 \tag{25}$$

Substituting (24) and (25) into (23), we get:

$$\begin{aligned}\dot{V}_2 &\le -c_1 \tanh\frac{z_1}{\eta}z_1 + z_2\left[z_1 + \hat{\theta}^{\mathrm{T}}\xi_1(Z_1) + \delta_1^* + bu - \dot{a}_2\right] \\ &\quad -\tilde{\theta}^{\mathrm{T}}\Gamma^{-1}\dot{\hat{\theta}} - (c_{21}-0.5)e^2 - |z_2 b\Delta u| - z_1\hat{\theta}^{\mathrm{T}}\xi_1(Z_1) \\ &\le -c_1 \tanh\frac{z_1}{\eta}z_1 + z_2\left[z_1 + \hat{\theta}^{\mathrm{T}}\xi_1(Z_1) + \delta_1^* + bv - \dot{a}_2\right] \\ &\quad -\tilde{\theta}^{T}\Gamma^{-1}\dot{\hat{\theta}} - (c_{21}-0.5)e^2 - z_1\hat{\theta}^{\mathrm{T}}\xi_1(Z_1)\end{aligned} \tag{26}$$

The final control law considering the hyperbolic tangent is:

$$v = \frac{1}{b}\left[-c_{20}\tanh\frac{z_2}{\eta} - e - z_1 - \hat{\theta}^{\mathrm{T}}\xi_1(Z_1) + \dot{\alpha}_2\right] \tag{27}$$

Among them, $c_{20}>0$, $\hat{\theta}$ is the estimated value of θ^*, and its online update form is as follows:

$$\dot{\hat{\theta}} = \Gamma[\xi_1(Z_1)z_1 - \sigma_1(\hat{\theta}-\theta_0)] \tag{28}$$

Among them, $\Gamma=\Gamma^{\mathrm{T}}>0$ is a constant matrix, $\dot{\hat{\theta}}$ is the derivative of the estimated value to avoid parameter drift. $\sigma_1>0$, and θ_0 is the initial value of θ.

$$\tilde{\theta}^{\mathrm{T}}(\hat{\theta}-\theta_0) = -\frac{1}{2}|\tilde{\theta}|^2 - \frac{1}{2}|\hat{\theta}-\theta_0|^2 + \frac{1}{2}|\theta-\theta_0|^2 \tag{29}$$

Lemma 1 (Polycarpou M M, Ioannou P A, 1996)**:** For any variable $x\in R$, the inequality $0\le|x|-x\tan(x/\eta)\le k\eta$ holds, where $\eta\in R^+$, the constant $k=0.2785$, and $k=e^{-(k+1)}$.

According to Lemma 1, we can obtain that

$$z_2 \le |z_2| \le z_2\tanh(\frac{z_2}{\eta}) + k\eta \tag{30}$$

Substituting (27), (28), (29), and (30) into (26) yields

$$\begin{aligned}\dot{V}_2 &\le -c_1\tanh\frac{z_1}{\eta}\cdot z_1 - c_2\tanh\frac{z_2}{\eta}\cdot z_2 - (c_{21}-0.5)e^2 \\ &\quad +z_2\delta_1^* + k\eta\delta_1^* - \frac{1}{2}|\hat{\theta}-\theta_0|^2 + \frac{1}{2}|\theta-\theta_0|^2 \\ &\le -c_1\tanh\frac{z_1}{\eta}\cdot z_1 - (c_2-\delta_1^*)\tanh\frac{z_2}{\eta}\cdot z_2 \\ &\quad -(c_{21}-0.5)e^2 + k\eta\delta_1^* - \frac{1}{2}|\hat{\theta}-\theta_0|^2 + \frac{1}{2}|\theta-\theta_0|^2\end{aligned} \tag{31}$$

At this point, let

$$\mu = [c_1, (c_2-\delta_1^*), (c_{21}-0.5), \frac{\sigma_\theta}{2\lambda_{\max}(\Gamma)}] \tag{32}$$

$$M = k\eta\delta_1^* + \frac{1}{2}|\theta-\theta_0|^2 \tag{33}$$

Then we have

$$\dot{V}_2 \le -2\mu V_2 + M \tag{34}$$

4. Stability Analysis

Lemma 2 (Li, 2012): If $V(t,x)$ is a positive definite function, and $\dot{V}\le -k_1V + k_2$, where $k_1\ge 0$ and $k_2\ge 0$ are bounded constants, then

$$V(t,x) \le \frac{k_2}{k_1} + (V(0) - \frac{k_2}{k_1})e^{-k_1 t} \tag{35}$$

Lemma 3 (Li, 2005)**:** If the function $f(t)$ is uniformly continuous, and $\lim_{t\to\infty}\int_0^t f(\tau)d\tau$ exists and is bounded, then $f(t)\to 0$ as $x\to\infty$.

Theorem 1 For the marine control system, under the conditions of Assumptions 1 and 2, the robust control law (27), the parameter adaptive law (28), and the internal stabilizing function α_2 can make the closed-loop system uniformly ultimately bounded. For a given $\mu_1\ge 0$, by adjusting the controller parameters, the tracking error can be made sufficiently small, $z_1 = y(t) - y_d(t)$ and $\lim_{t\to\infty}|z_1(t)|\mu_1$.

Proof: According to Lemma 2, from Equation (34), we have:

$$0 \le V_2 \le \frac{M}{2\mu} + [V_2(0) - \frac{M}{2\mu}]e^{-2\mu t} \tag{36}$$

From the above derivation, it can be seen that $[V_2(0) - \frac{M}{2\mu}]$ exhibits an exponential decay characteristic. Thus, as $t \to \infty$, $\lim_{t\to\infty} \int [V_2(0) - \frac{M}{2\mu}]dt$ exists and has a limit. It is known that $V_2(t)$ is bounded, and for all t, $m \le V_2(t) \le M$. Meanwhile, $\dot{V}_2$ is bounded, so $V_2(t)$ is uniformly continuous. Therefore, by Lemma 3, we can obtain:

$$\lim_{t\to\infty} V_2 = \frac{M}{2\mu} \tag{37}$$

That is, when a function itself is bounded and its derivative is also bounded, the function is uniformly continuous. For any $\varepsilon \ge (\frac{M}{\mu})^{1/2}$, there exists a constant $T \ge 0$ such that when $t \ge T$, the tracking error satisfies $\lim_{t\to\infty} |z_1(t)| \le \varepsilon$. By appropriately selecting parameters c_1、c_2、c_{21}、σ_θ、θ_0, $(\frac{M}{\mu})^{1/2}$ can be made arbitrarily small. Therefore, the latter part of the theorem is proved.

5. Simulation Verification

In this section, MATLAB software is employed to conduct simulation studies in order to verify the effectiveness of the proposed controller. The simulations are based on the "Yulong" training vessel of Dalian Maritime University (Li, 2009). The principal particulars of the Yulong vessel are as follows: the length overall is 126.0 m, the beam is 20.8 m, the full-load draft is 8.0 m, the block coefficient is 0.681, and the service speed is 7.7 m/s.

To evaluate the performance of the adaptive hyperbolic-tangent control algorithm proposed in this study, a complete ship heading control simulation platform is constructed within the MATLAB environment. The total simulation time is set to 1200 s. The model incorporates the combined effects of environmental disturbances such as wind, waves, and ocean currents, thereby simulating various sea states. The initial heading deviation is set to 30°. The RBF neural network employed in the controller contains 25 nodes, uses a Gaussian activation function, and adopts center vectors uniformly distributed within the interval [−4, 4] with a width parameter of 2. The learning rate is set to 0.01, the initial weights are zero, and the weight updating process follows the adaptive law specified in equation (28).

All parameters are tuned through multiple experiments to achieve a balance between response speed and system smoothness. The identified parameters of the ship Nomoto model are obtained as follows: $c_1 = 0.25$, $c_2 = 200$, $c_{21} = 0.5$, $\varepsilon = 0.01$, $\Gamma_1 = diag\{0.001\}$, $\Gamma_2 = diag\{0.01\}$, $T = 1200$, the initial value of e is set to 20.

The simulation results are presented as follows:

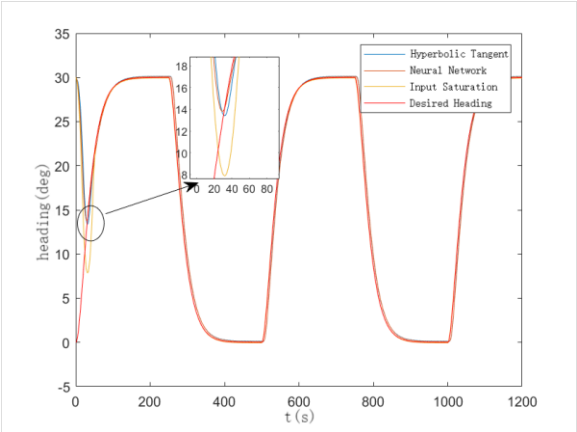

Fig. 1 Time response of curve of ship course

Figure 1 illustrates that the proposed algorithm reduces the heading-angle error to within 0.5° w ithin 40 s, demonstrating a fast convergence rate without noticeable overshoot. Under the same in itial conditions, when the hyperbolic-tangent corr ection term is not applied, the system still exhib its a steady-state error of approximately 2° at 6 0 s. This comparison indicates that the nonlinear function introduced in this study provides signifi cant advantages in limiting control output magni tude and suppressing oscillations.

As time progresses, the heading response curve exhibits a smooth asymptotic behavior, confirming that the controller achieves satisfactory dynamic performance. Figure 1 includes the heading trajectories obtained using the proposed hyperbolic-tangent control, a conventional neural- network-based controller, a traditional input- saturation controller, and the desired heading. Although initial fluctuations are observed, the actual heading generated by the proposed method rapidly converges to the desired trajectory and maintains an almost negligible error after stabilization, thereby validating the accuracy and effectiveness of the developed heading-tracking system.

Compared with the heading response under the traditional neural network controller, the proposed method achieves a faster response. Relative to the controller that considers only input saturation, the proposed approach exhibits superior tracking performance with smaller deviation angles, demonstrating enhanced capability in accurately controlling ship heading under complex operating conditions.

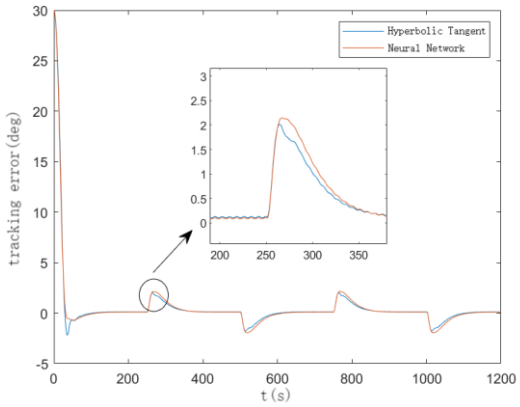

Fig. 2 Time-history curve of ship tracking error

In Figure 2, it can be observed that the tracking error remains within ±0.3° throughout the entire simulation, and no noticeable periodic oscillation occurs during the steady-state phase. It is worth noting that an instantaneous spike appears at approximately 270 s, corresponding to the moment when a sudden disturbance is introduced. The system subsequently restabilizes within about 60 s, demonstrating the rapid disturbance-rejection capability provided by the adaptive term and the neural network compensation. This characteristic is particularly important for autonomous vessels, as it significantly enhances continuous controllability under wind, wave, and current disturbances.

Figure 2 shows the ship's heading-tracking error. From the overall trend, both the hyperbolic-tangent controller and the traditional neural-network-based controller maintain low error levels for most of the simulation period, achieving effective heading tracking. The advantages of the proposed method are prominent: at the initial stage, the heading-tracking error rapidly converges to nearly zero, exhibiting a faster convergence rate; during the steady-state phase, the proposed method yields smaller error fluctuations, resulting in a more stable heading response.

From a local perspective, as shown in the enlarged sub-region, the peak error produced by the proposed method is lower than that of the traditional neural-network controller. This indicates stronger suppression of error growth when subjected to local disturbances, and thus higher tracking accuracy.

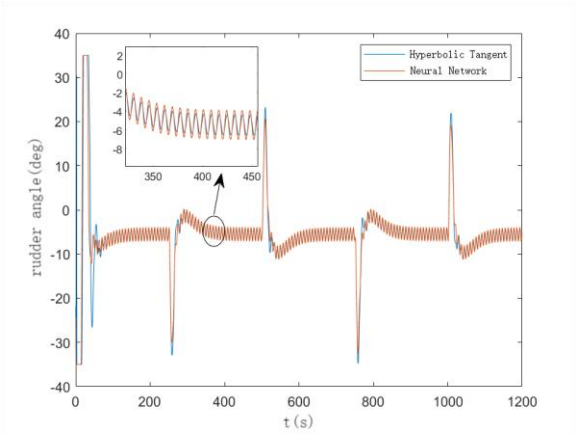

Fig. 3 Time response of ship rudder angle

Figure 3 presents the time history of the rudder-angle input. Overall, the rudder-angle trajectories of the hyperbolic-tangent controller and the neural-network-based controller exhibit similar trends during most periods of the simulation. However, the proposed method produces smaller rudder-angle fluctuations and smoother adjustments, which helps reduce unnecessary actuator motion and mechanical wear.

In the locally enlarged view, the traditional neural-network controller displays pronounced high-frequency oscillations in the rudder input, whereas the rudder-angle curve generated by the proposed method remains smooth, with high-frequency components effectively suppressed. This indicates that the proposed controller achieves more stable and precise rudder control.

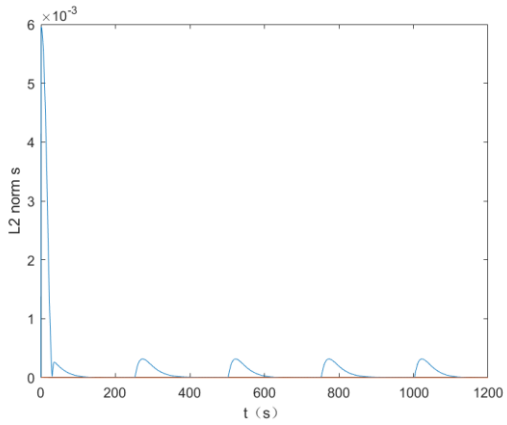

Fig. 4 Time response of the norms of the NN weights

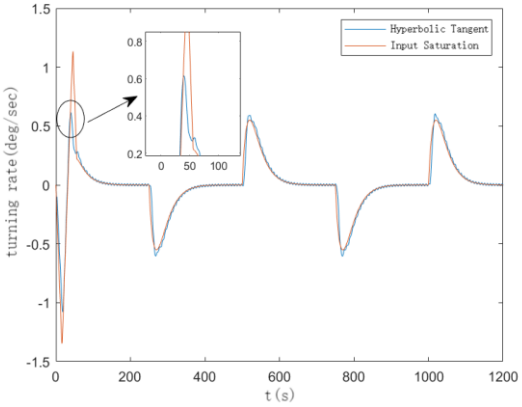

Fig. 5 Time response of ship yaw rate

Figure 5 illustrates the yaw-rate response. From the overall trend, the yaw rate exhibits certain oscillations during the initial stage of control, but it gradually stabilizes after approximately 60 s, with the oscillation amplitude decreasing to about 0.3°/s Combined with the Lyapunov-based analysis, this behavior reflects the progressive dissipation of system energy, which is consistent with the theoretical derivation. By introducing the saturation-assisting mechanism and the hyperbolic-tangent function, the control input is effectively constrained within the allowable operating range, thereby ensuring the global stability of the closed-loop system.

Based on the comprehensive simulation results, several conclusions can be drawn:

The nonlinear characteristics of the hyperbolic-tangent function serve as a soft constraint within the control law, enabling smooth transitions of the control signal and effectively suppressing high-frequency oscillations. The adaptive learning mechanism of the RBF neural network allows rapid weight updates under external disturbances and parameter variations, thereby achieving dynamic compensation for model uncertainties. The designed robust controller has a simple structure, involves only a few tunable parameters, and is easy to implement in engineering applications.

The simulation results verify that the proposed method not only guarantees system stability and fast convergence but also maintains excellent control performance under complex marine environmental conditions.

6. Conclusion

In this study, an auxiliary system is introduced to address the rudder-angle saturation inherent in ship steering, effectively constraining the rudder input within ±35° and ensuring stable system operation. To handle the nonlinear characteristics of the ship heading dynamics, a hyperbolic-tangent function is incorporated into the control law. Leveraging its smoothness, bounded output, and

inherent ability to suppress chattering, an adapti ve control method is developed based on Lyapu nov theory and the backstepping framework. Th e nonlinear mapping capability of the hyperbolic -tangent function enables dynamic accommodatio n of system uncertainties, thereby eliminating th e need for complex conventional modeling proce dures. This approach not only simplifies the con struction of fuzzy-rule bases and parameter tunin g but also guarantees satisfactory control perfor mance through the intrinsic properties of the hy perbolic-tangent function, allowing the tracking e rror to meet the desired precision. Consequently, accurate and stable heading control is achieved, enabling the vessel to follow a prescribed route even under complex sea conditions.

Compared with traditional control approaches, t he proposed method attains high-accuracy headin g tracking and strong disturbance rejection witho ut relying on extensive parameter identification. The control law is mathematically rigorous whil e maintaining practical engineering feasibility, m aking it particularly suitable for ship heading sy stems subject to input saturation constraints. Sim ulation results demonstrate that the strategy signi ficantly reduces the initial heading deviation wit hin 40 s, maintains the steady-state error within ±0.5°, and avoids both rudder-angle violations a nd system oscillations. The neural network offer s online approximation of unknown nonlinearitie s, thereby enhancing the controller's adaptive ca pability, whereas the hyperbolic-tangent function introduces a smooth limiting effect that eliminat es discontinuities and preserves the differentiabili ty of the control input. The combination enhanc es control accuracy, improves robustness, and str engthens disturbance resistance. Stability analysis further confirms that the closed-loop system sati sfies the property of uniform ultimate boundedne ss.

Overall, this work provides a feasible theoretic al framework and valuable engineering reference for the design of intelligent ship control systems.

References

Du J L, Hu X, Sun Y Q. (2020), Adaptive Robust Nonlinear Con340 trol Design for Course Tracking of Ships Subject to External Disturbances and Input Saturation . IEEE Transactions on Systems Man Cybernetics-Systems, Vol. 50, pp. 193-202.

Jia W, Wang N, Wu H. (2024), Adaptive Fuzzy Pat h Following for Autonomous Underactuated Ships: A Hyperbolic-Tangent Fixed-Time Control Approach. //2 024 IEEE 27th International Conference on Intelligent Transportation Systems (ITSC). IEEE, pp. 3962-3967.

Jia, X. , & Yang, Y. (1997), Mathematical Models of Ship Motion. Dalian: Dalian Maritime University Press.

Le T T. (2021), Ship heading control system using neural network. Journal of Marine Science and Techn ology, Vol. 26, No. 3, pp. 963-972.

Li, J. (2012), Design of Ship Heading Autopilot Co nsidering Input Saturation. Dalian: Navigation College, Dalian Maritime University.

Li T S, Wang D, Feng G, et al. (2009), A DSC A pproach to Robust Adaptive NN Tracking Control for Strictfeedback Nonlinear Systems . IEEE Transactions on Systems, Man and Cybernetics- Part B: Cyberneti cs, Vol. 40, No. 3, pp. 915-927.

Li T S. (2005), Nonlinear Design Methods for Strai ght-Line Ship Trajectory Control. Dalian: Dalian Mari time University.

Liu H, Zhou X, Tian X, et al. (2024), Adaptive sel f-structuring neural network tracking control for unde

ractuated USVs with actuator faults and input saturati on. Ocean Engineering, Vol. 309, pp. 118535.

Liu S, Zhang G, Zhang W, et al. (2022), Robust fu zzy dynamic surface formation control for underactua ted ships using MLP and LFG. Systems Science & Control Engineering, Vol. 10, No. 1, pp. 272-281.

Liu S, Zuo Y, Li T, et al. (2024), Adaptive Compo site Fixed- time RL Optimized Control for Nonlinear Systems and Its Application to Intelligent Ship Autop ilot. IEEE Transactions on Artificial Intelligence.

Mu D D, Wang G F, Fan Y S, et al. (2019), Adaptive Course Control Based on Trajectory LinearizationControl for Unmanned Surface Vehicle with Unmodeled Dynamics and Input Saturation. Neurocomputing, VOL. 330, pp. 1-10.

Ning J, Chen H, Li W, et al. (2021), DSC-ESO Ap proach to Robust Sliding Model Control for Ship's C urve Trajectory Tracking. IEEE Access, Vol. 9, pp. 3 0712-30720.

Polycarpou M M, Ioannou P A. (1996), A robust adaptive nonlinear control design. Automatica, Vol. 32, No. 3, pp. 423–427.

Sui J, Bai C, Song C, et al. (2024), Nonlinear Inno vation Identification for Norrbin Mathematical Model Via Actual Ship. //2024 36th Chinese Control and D ecision Conference (CCDC). IEEE, pp. 572-577.

Sun, W. , Bu, R. , & Liu, Y. (2020), Ship Heading Control with Roll-Suppression Function Using PID D ifferential Compensation. Journal of Shanghai Maritim e University, Vol. 41, No. 03, pp. 19–24.

Suyama R , Satoh S , Maki A. (2024), Nonlinear s teering control law under input magnitude and rate c onstraints with exponential convergence. Journal of M arine Science and Technology, Vol. 29, No. 4, pp. 1-14.

Xu, G. , & Zhang, X. (2013) A Review of Researc h on Ship Autopilot Systems. Shipbuilding of China, Vol. 54, No. 02, pp. 191–200.

Xu M , Gong C. (2024), Finite-Time Disturbance O bserver-Based Adaptive Course Control for Surface S hips. [J]. Sensors (Basel, Switzerland), Vol. 24, No. 15, pp. 4843-4843.

Zhang H, He Z, Wang G, et al. (2025), Ocean Cur rents Compensation-Based IAILOS-ROESOs Guidance and Adaptive Sliding Mode Path Following Control f or Unmanned Surface Vehicles. International Journal of Adaptive Control and Signal Processing, Vol. 39, No. 4, pp. 692-708.

Zhang, Y. (2004), Proof and Application of Young's Inequality. Henan Science, No. 01, pp. 23–29.

Zhou M, Zhang X, Deng X. (2024), Tracking control problem of nonlinear strict-feedback systems with input nonlinearity : An adaptive neural network dynamic surface control method. PloS one, Vol. 19, No, 10, pp. e0312345.

Received **11 November 2025**

1st Revised **25 December 2025**

Accepted **05 January 2026**